で5分間，PBTで5分間それぞれ振盪した後，再度PBTに置換し5分間振盪した．Proteinase K/PBT溶液（2 μg/ml）に置換し，37℃で15分間振盪した．その後，glycine（2 mg/ml）/PBT溶液に置換後，室温で5分間，PBTで5分間2回振盪した．2％gluteraldehyde＋4％paraformaldehyde を含むPBTに置換し，20分間再固定した．その後，PBTに置換し5分間振盪した（2回繰り返す）．次いでPBT中68℃で50分間熱処理した．十分に冷却したPBTに置換し，氷上で5分間振盪した．6％H₂O₂/methanol溶液に置換し，氷上で1時間振盪した．その後，PBSで5分間，PBTで5分間振盪し，68℃のpre-hybridization mix（50％formamide，5×SSC pH 7.0，50 μg/ml tRNA，1％SDS，50 μg/ml heparin）に置換し，1時間振盪した．

Digoxigenin（DIG）- labeled RNA probe（0.35 μg）を含むpre-hybridization mix溶液（0.7 ml）に置換し，68℃で一晩hybridizationを行った．その後，Hybridization Wash Solution 1（5×SSC，50％formamide，1％SDS）に置換し振盪した．再度新たなHybridization Wash Solution 1に置換し，68℃で30分間振盪して洗浄を行った．その後，Hybridization Wash Solution 2（2×SSC，50％formamide，0.1％Tween20）で5分間，次いで同じ液を用いて68℃で30分間，さらにTBST（100 mM Tris-HCl，pH 7.5，150 mM NaCl，0.1％Tween 20）で室温5分間を3回繰り返し，ブロッキング溶液（1.5％Blocking Reagentを含むTBST）で60～90分間，それぞれ振盪した．最後にブロッキング溶液を除き，抗体を加え4℃で一晩抗体反応を行った．

TBSTに置換し5分間振盪を4回行った．新たなTBSTに置換して，30分間振盪を8回，NTMT（0.1 M NaCl，0.1 M Tris-HCl, pH9.5，50 mM MgCl₂，0.1％Tween 20）に換えて3回，10分間振盪による洗浄を行った．その後，NTMTを発色液（NBT：4-nitro blue tetrazolium chloride＋BCIP：5-bromo-4- chloro-3- indolyl-phosphateを含むNTMT）に換え，発色反応を

開始した．発色開始10分後から発色状況を確認し，発色が完了したところでPBTに置換し，5分間振盪を3回行い，発色反応を停止した．次に50％ethanol/PBTに置換し，5分間振盪後100％ethanolに換え1.5～3時間振盪した．その後，50％ethanol/PBTで5分間，PBTで5分間振盪した後，撮影まで遮光して4℃で保存した．

切片でのISHはWhole-Mount ISHの手法に準じて行った．固定した胚を脱水後にパラフィン包埋し，厚さ7 μmで切片を作製した．脱パラフィン処理して再水和後，Proteinase K（0.5 μg/ml）/PBT溶液に置換し，37℃で10分間，酵素処理を行った．その後，室温でglycine（2 mg/ml）/PBT溶液に置換して5分間，PBTで2回5分間振盪した．4％PFA/PBT溶液に置換し，再固定を20分間行った．その後，PBTに置換し5分間3回振盪した．0.1 M triethanolamine中で無水酢酸を加えて15分間アセチル化を行った後，PBTに置換して5分間5回振盪した．Whole-Mount ISHで用いたpre-hybridization mixに終濃度10％dextran sulfateを加えたものを切片ISHで使用し，65℃で1時間処理した．DIG-labeled RNAプローブ（1 μg/ml）を含むpre-hybridization mixに置換し，65℃で16～17時間hybridizationを行った．Hybridization Wash Solution 3（2×SSC, pH7.0，50％formamide，0.1％SDS）に置換し，65℃で20分間4回洗浄を行った．その後，0.2×SSC＋0.1％Tween 20に置換し65℃で20分間4回洗浄した．さらにTBSTで室温5分間2回，ブロッキング溶液中で15℃，1時間，それぞれ振盪した．ブロッキング溶液を除き，抗体を加えて15℃で2時間抗体反応を行った．TBSTに置換し，10分1回，5分6回振盪した．次にNTMTに置換し，5分間2回の振盪による洗浄を行った．その後，NTMT中に発色基質（NBT＋BCIP）を含む溶液に換え，発色反応を開始した．発色液はWhole-Mountの場合の1/10の濃度を用いた．発色時間は発色の状態を確認しながら1～2日間室温で行った．発色停

止後に0.1% Nuclear fast red/5% 硫酸アルミニウム水溶液で核を染色した.

5. Western blotting

　資料の調製，及び western blotting は笹岡の手法に準じて行った[12]. 用いた抗体は次の通り. 抗 MyHC 遅筋型 (Sigma)：1/4,000, peroxidase で標識した anti-mouse IgG 抗体 (Sigma)：1/20,000. 検出したシグナルを Densitograph (ATTO) を用いて数値化した.

結　　　果

1. MSTN とその受容体の発現パターン

　四肢が形成される段階で MSTN の発現パターンを調べると，皮筋節で発現が始まり，体幹部から四肢へ前駆細胞の移動が起きている場所で発現が維持されている (Figs. 1, 2). その一方で，ActRIIA の発現は MSTN より少し早くから発現が始まり，発現の継続も MSTN よりは長い. すなわち，ニワトリ胚の肢芽では発生ステージ23から MSTN の発現が始まり，四肢の筋肉での発現はステージ24でピークにな

る. その後，ステージ25までは発現が見られるが，ステージ26では消失する.

　一方，ActRIIA の発現は皮筋節や肢芽での Pax7 の発現と重なり，ステージ23ではすでに有意な発現が見られる. その後，ステージ24-26で最も強く発現が見られ，ステージ29-30までは発現が持続する.

　ActRIIB については，ステージ23-26で皮筋節，肢芽の筋肉部位での発現は全く見られず，ステージ23-25で神経管，肢芽の背側間充織などでの発現が見られるが，肢芽での発現はステージ27以降では弱くなる.

　このように，MSTN の発現は ActRIIA とはオーバーラップしているが，ActRIIB とはオーバーラップせず，その一方で MSTN の発現は一過性であることが判明した (Table 1).

　筋芽細胞へ分化する前駆細胞である衛星細胞のマーカーであると言われている Pax7 の発現[13]は,神経管背側での発現に加えて,ステージ23前後から皮筋節や肢芽の筋肉塊周辺で強い発現が見られる (Figs. 1, 2). ここでの発現はステージ26-27まで継続し，ステージ29-30では筋肉塊での発現は低下するが，発現している細

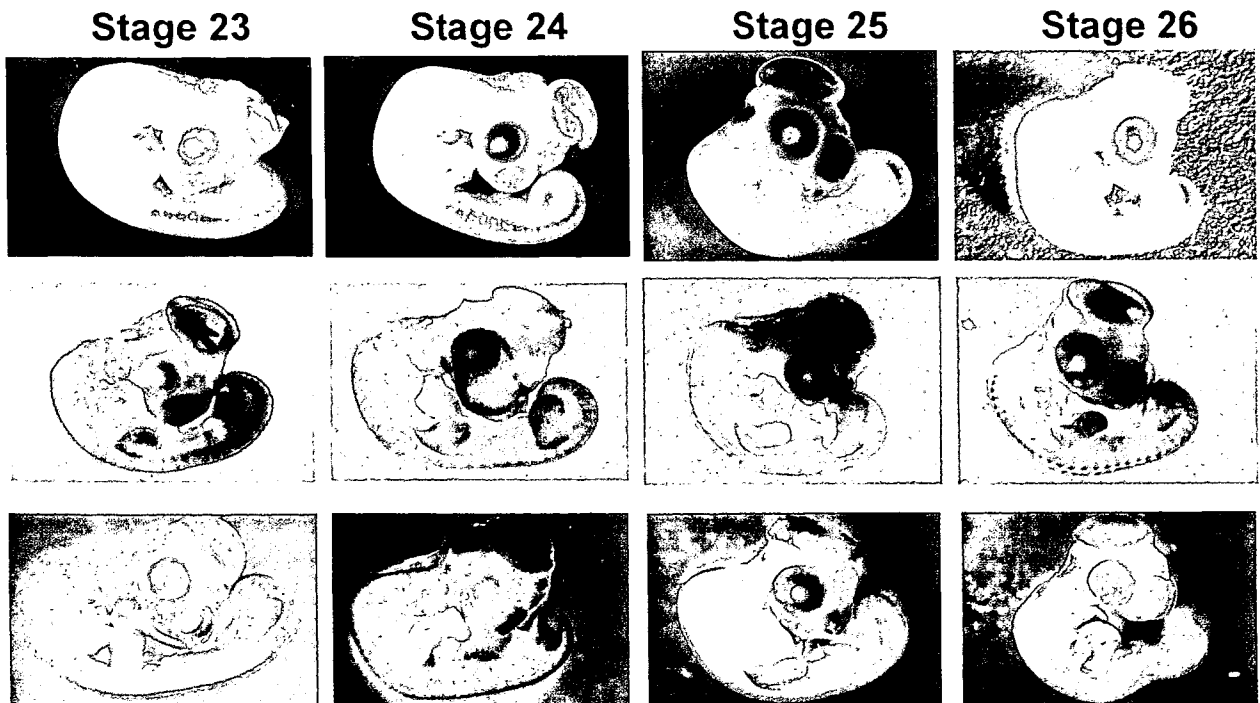**Stage 23**　　**Stage 24**　　**Stage 25**　　**Stage 26**

Fig. 1. Expression patterns of MSTN, ActRIIA, and ActRIIB during chick embryogenesis, as revealed by whole-mount in situ hybridization at stages 23 to 26. Top, MSTN ; middle, ActRIIA ; bottom, ActRIIB.

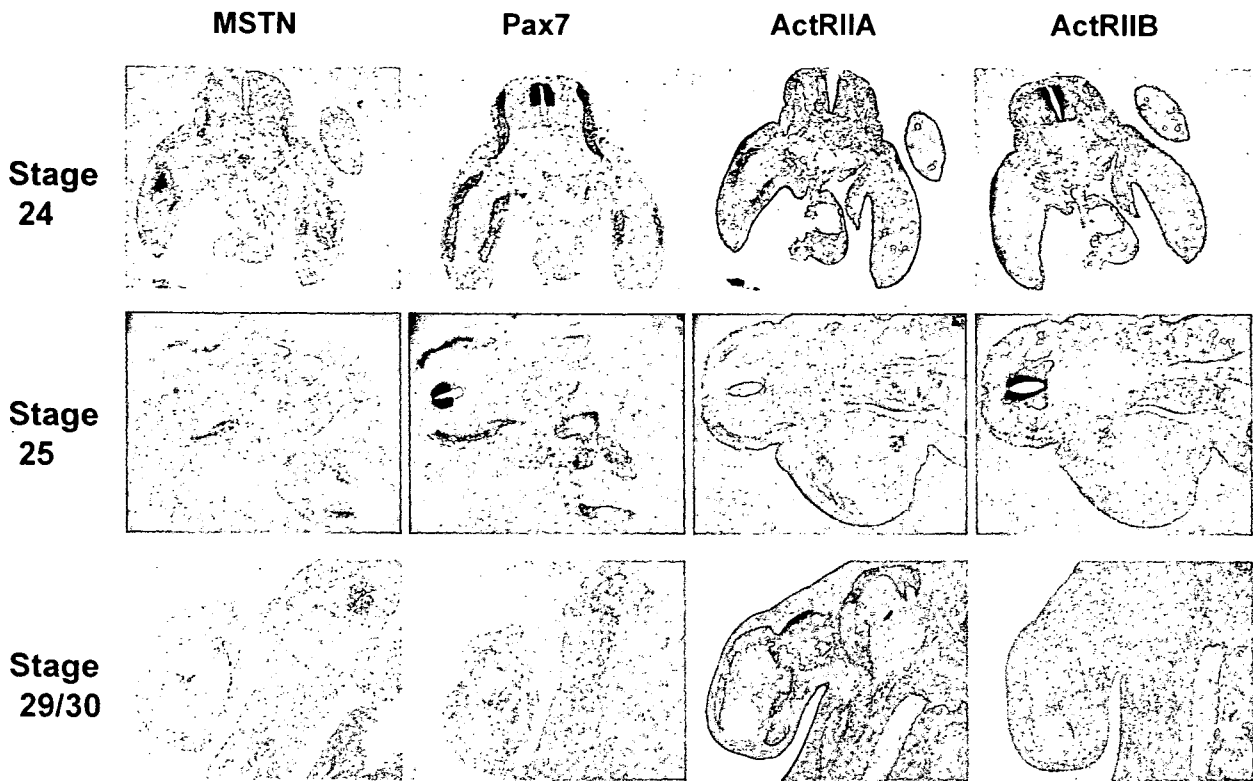| MSTN	Pax7	ActRIIA	ActRIIB

Stage 24

Stage 25

Stage 29/30

Fig. 2. Expression pattern of MSTN, Pax7, ActRIIA, and ActRIIB during chick embryogenesis, as revealed by section in situ hybridization at stages 24 to 30. ActRIIA, but not ActRIIB, is expressed in myogenic cells during migration into the limb bud with MSTN and Pax7.

Table 1 Summary of expression pattern in the chick embryos at stage (St) 23 - 26.

Probe (Gene)	Site	Developmental Stage				Comment
		St 23	St 24	St 25	St 26	
Myostatin	Limb bud	+	+ +	+	—	
	Myotome	+	+	±*	±*	*Partial
	Neural tube	—	—	—	—	
Pax7	Limb bud	+	+ +	+ +	+ +	
	Myotome	+ +	+ + +	+ +	+ +	Intense at St 24
	Neural tube	+ +	+ +	+	+	Dorsal half
ActRIIA	Limb bud	+	+ +	+ +	+ +	
	Myotome	+	+ +	+ +	+ +	
	Neural tube	—	—	+	+	
ActRIIB	Limb bud	+	+	+	+	Weak in myoblast
	Myotome	±	+	±	±	Intense at St 24
	Neural tube	+ +	+ +	+	+	Intense at St 23, 24

—, no signal ; ±, weak ; +, moderate ; + +, intense ; + + +, very intense signals.

胞が筋肉塊の中に部分的に散在するようになる．

皮筋節での MyHC の発現はステージ25から認められるようになり，速筋型では軸下の細胞に限局しているが，遅筋型では軸上領域まで発現が見られる（**Fig. 3**）．その後，肢芽へ移動した筋芽細胞での発現が始まるが，その発現領域は速筋型の方が広範囲である．従って，MSTN の発現は時間的，空間的に遅筋の発現と関連している可能性がある．

2．MST-MAT, MST-PRO, AR2A-DN, AR2B-DN の DF-1 細胞での発現

全長 cDNA に HA タグ用の配列を追加してヒト MSTN タンパク質の産生を試みたが，分泌効率もプロセシングの効率も極めて低い．それゆえアミノ酸（aa）19-266（MST-PRO）と aa 267-375（MST-MAT）の間で分断し，それぞれ C 末端側に HA タグを付けて別々に発現した．しかし，この場合でも細胞内にタンパク質は認められるが，培養液中へはほとんど分泌されていなかった．

一方，細胞外ドメインのみの配列に V5 タグを付けたヒト ActRIIA の aa 20-137（AR2A-DN）も，ヒト ActRIIB の aa 23-133（AR2B-DN）も培養液中への分泌が極めて高く，特に AR2A-DN では合成されたタンパク質がほとんど分泌されており，細胞内への残存はあまり見られなかった．このように，AR2A-DN も AR2B-DN も産生タンパク質は効率よく分泌されているのが確認された．この結果はシグナル配列の違いによるものと推測される．CM 中への産生効率は AR2B-DN＞AR2A-DN であった．

次に，ActRIIA と ActRIIB のシグナル配列（SP）に HA タグ配列を持つ MST-PRO と MST-MAT をつなぎ，AR2A(SP)-PRO，AR2A(SP)-MAT，または AR2B(SP)-PRO，AR2B(SP)-MAT として発現させた．その結果，タンパク質産生のタグ抗体による検出では，どちらのシ

Fast MyHC
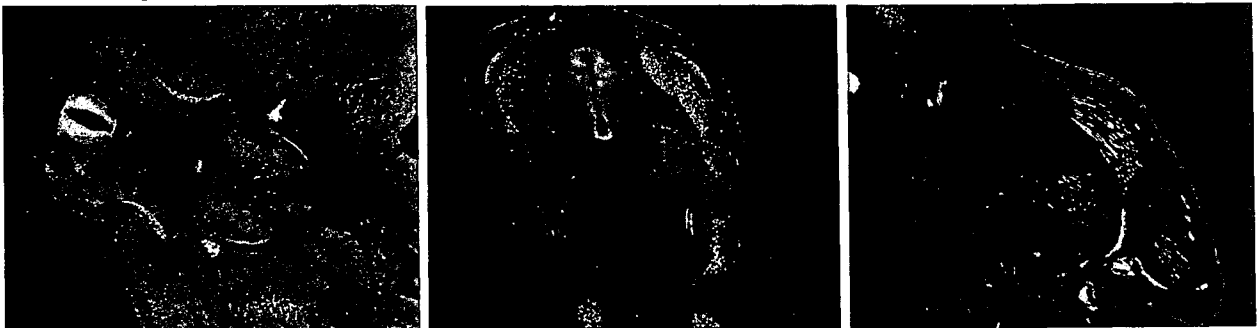
Slow MyHC

| Stage 25/26 | Stage 29/30 | Stage 29/30 |

Fig. 3. Expression pattern of slow and fast myofiber MyHC during chick embryogenesis, as revealed by immunofluorescent staining. AlexaFluor 594-labeled secondary antibody detects primary antibody bound to fast muscle MyHC (top) and slow muscle MyHC (bottom). Cell nuclei were counterstained with DAPI.

グナル配列の場合でも効率よく MST-PRO, MST-MAT のいずれについても CM 中へ十分量が産生されていた．産生量は AR2B(SP) -PRO > AR2A(SP) -PRO > AR2B(SP) -MAT > AR2A (SP)- MAT の順であった．

これら ActRII のシグナル配列を持つクローンはいずれも RCAS ベクターへ組換えてウイルスとしての発現を試みた．

3．筋分化における MSTN 作用の阻害効果

マウス筋芽細胞 C2C12 を用いて MSTN 作用を検証した．2％ウマ血清または2.5％ウシ胎児血清で分化誘導をかけて検定した時，組換えタンパク質（rMST-MAT）に対する応答が悪く，50〜400 ng/ml では MyHC 抗体での染色で見る限りほとんど筋分化の抑制効果は見られなかった．10％ウシ胎児血清存在下での細胞増殖に対する抑制効果も，M 期のマーカーである histone H3-P 抗体でのラベリング[14]で調べて差は見られなかった．細胞分化の誘導をかけたとき，C2C12 では MyHC の遅筋型の方が速筋型よりも優先して多数出現してくる．MSTN 阻害の効果は速筋型に対して効果が現れやす

く，遅筋型ではあまり効果がないと言われているので，C2C12 は MSTN 作用の検定系として感度が悪く，あまり適していないと考えられる．

次に，ニワトリ胚の初代培養細胞 CLM を用いて検定した．その結果，rMST-MAT 50 ng/ml で筋分化の抑制が見られ，その効果は速筋型に対して顕著であった（**Fig. 4**）．DF-1 細胞で発現した AR2B-DN も AR2A-DN もこの細胞へ加えると分化の促進効果が見られた（**Fig. 5**）．このことは遅筋型 MyHC で調べた Western blotting でも確認された（**Fig. 6**）．

MST-PRO と AR2A-DN，AR2B-DN では筋分化促進活性に違いがあるかどうかをさらに確認する必要があるので，これらを RCAS に組み込んで発現した．CLM での検定では AR2A - DN が有効である証拠が得られている．最終的には生体内で発現させるために，ウイルスベクターを用いた持続的な発現法を開発する必要がある．
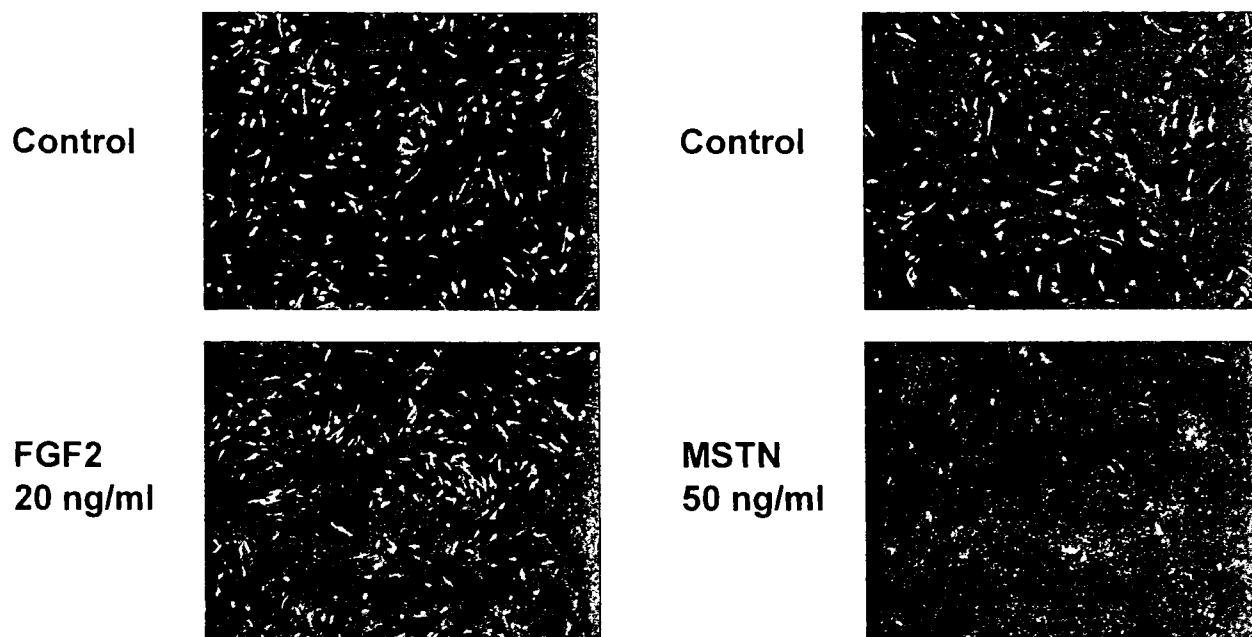
考　　察

発現パターンから，MSTN の筋分化に対す

Fig. 4. Effect of recombinant FGF2 and MSTN proteins on myogenic differentiation of chicken myoblasts during high-density primary culturing. Limb bud cells from a stage 24 embryo were cultured for three days in the presence or absence of recombinant proteins, and fixed for immunofluorescent staining against fast muscle MyHC (AlexaFlour 594 label), followed by counterstaining with DAPI.
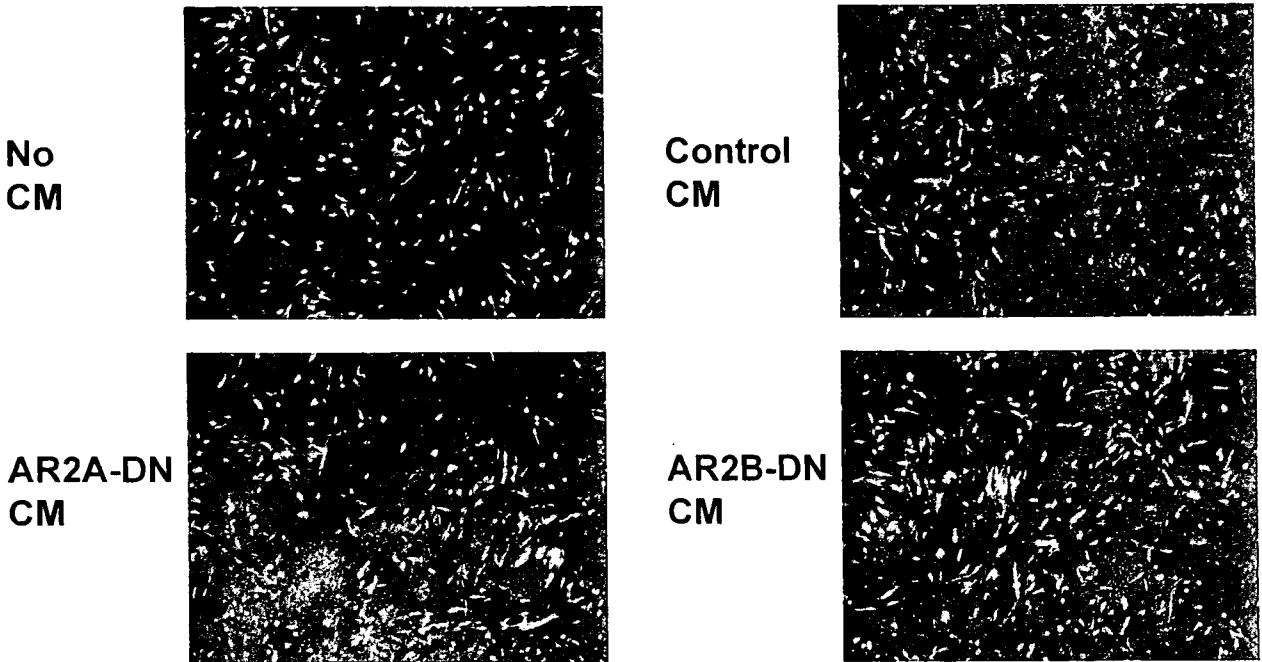
Fig. 5. Effect of AR2A-DN and AR2B-DN proteins on myogenic differentiation of chicken myoblasts during high-density primary culturing. Limb bud cells from a stage 24 embryo were cultured for three days with the serum-free conditioned medium (CM) from DF-1 cells expressing AR2A-DN and AR2B-DN. Control cells were cultured with or without control CM. Cells were fixed for immunofluorescent staining against fast muscle MyHC (AlexaFlour 594 label), followed by counterstaining with DAPI.
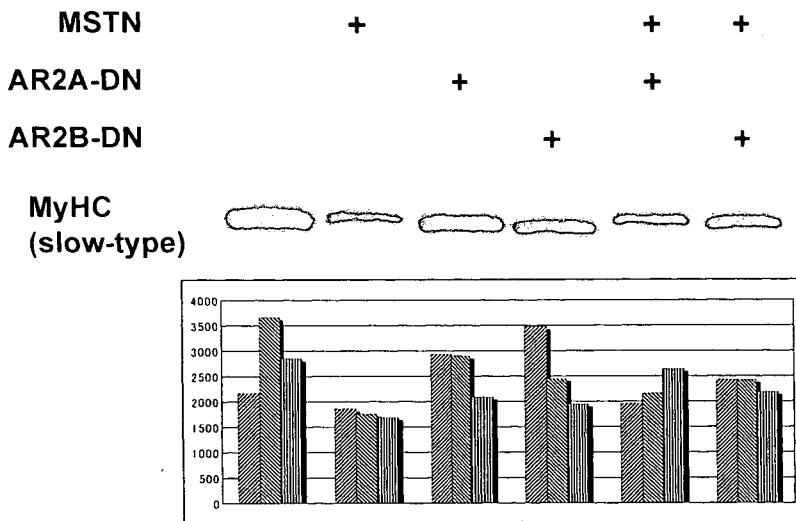

Fig. 6. Competitive effect of AR2A-DN and AR2B-DN from the conditioned medium (CM) against recombinant MSTN during myogenic differentiation of chick primary myoblasts. Limb bud cells from a stage 24 embryo were cultured for three days in the presence or absence of CM and recombinant MSTN. Myogenic differentiation was determined by Western blotting of total protein with anti-slow muscle MyHC antibody, and was detected with a peroxidase-labeled secondary antibody. The relative intensities of the bands were densitographed and typical results are shown at the top. The columns at the bottom indicate the relative intensities of the bands, determined in three independent experiments.

駆細胞が最初に皮筋節から遊走するのに一致して MSTN の発現が見られる．一方，類似の構造を持つ ActRIIB は MST-MAT との結合親和性は高いが，筋肉に分化する細胞で全く発現していない．従って，筋分化に対する特異的な効果を得るためには，MSTN が ActRIIA へ結合するのを遮断することが重要であり，一方で ActRIIB へのシグナルを遮断する場合には神経細胞などに対して望ましくない効果が現れる可能性がある．欠損型受容体の MSTN に対する阻害活性が高いかどうかのみで判断するのではなく，他のシグナル分子に対する影響が出にくいという点も考慮して，MSTN 阻害活性を評価すべきである．

MSTN タンパク質の産生，分泌はシグナルペプチドに大きく依存している．すなわち，MSTN 自身のシグナル配列では培

る抑制作用は主に ActRIIA を介していると考えられる．すなわち，筋肉細胞へと分化する前

養液中への分泌効率が低く，元来 MSTN は生合成された細胞内に大部分が留まり，極めて少量しか分泌されていない．MSTN の生理活性は C 末端側のペプチド MST-MAT にあり，N 末端側 MST-PRO はその活性を阻害する．そのためプロセシングを受けていなければ受容体との結合活性はない[4),15)]．さらに，細胞によっては切断の活性が極めて低い．以上のように，転写された MSTN mRNA から MST-MAT タンパク質が分泌されて標的細胞で作用するまでの道筋には多くの段階がある．この活性化に至る各段階で調節を受けているので，それぞれの段階を妨げることで生理活性を調節することができる．筋芽細胞で発現している MSTN 自身の自己増殖抑制，分化抑制作用を MST-MAT との結合タンパク質を使って阻害するのみならず，プロセシングの阻害や分泌の阻害によっても達成することができるので，この方面での開発も必要である．

　MST-PRO および Follistatin とその関連ペプチドは MST-MAT に直接結合してその受容体への結合を阻害することで筋分化を促進する作用があるが[16)～18)]，このような作用は MST-MAT の膜受容体の細胞外ドメインを用いても達成することができる[5),8)]．リガンドが最初に結合する受容体は ActRII であるが，ここで示したように B 型が神経に分化する細胞で発現しているのに対し，A 型が筋分化の過程では優先して発現している．MST-MAT との結合親和性は B 型の方が高いが[5)]，欠損型の AR2A - DN でも AR2B-DN と同等の筋分化促進作用が確認された．発現パターンを考慮すると，AR2B-DN では神経系の発生に対する影響が現れると思われるが，AR2A-DN では MSTN 活性に対する効果が筋肉組織に対して特異的に現れるであろうと推測される．

　これらの阻害ペプチドの過剰発現による遮断作用を MSTN に対して十分発揮するには，それを恒常的に発現し，供給し続けなければならない．MSTN 阻害抗体やプロペプチドを用いた実験動物での効果はタンパク質製剤の直接投与が行われているために 1 回に大量を使用する必要があった．臨床研究でも同様である．この点が MSTN 阻害タンパク質による治療法開発の大きな障害となっている．

　これを克服する 1 つの方法として，ニワトリのレトロウイルス由来のベクターである RCAS とその受容体をコードする tva 遺伝子を利用する方法がある[19)]．複製可能な RCAS ベクターはこれまでにニワトリ胚などの実験系で研究用に使用され，その安全性が確認されてきた[20),21)]．これらは鳥類の細胞では増殖複製可能型の感染性ウイルスであり，力価の高い組換えウイルスが効率よく産生できる．しかし，哺乳動物の細胞へこのウイルス粒子が感染するためには，細胞膜受容体をコードする tva 遺伝子の産物がウイルス受容体として必要であるが，これはマウスやヒトのゲノムには存在せず，鳥類に固有である．さらに，この tva 遺伝子をマウス細胞などへ導入した場合でも，RCAS の感染は起こるが，ウイルス遺伝子の構造の違いのためウイルスの複製が極めて悪く，実質上複製が起こらないことが確認されている[22),23)]．この発現系をヒトへ応用する方法としては，間充織系の幹細胞などへ tva を導入して強制発現させ，細胞をウイルス感受性にしてから患者へ戻す．その後，AR2A-DN を持つ RCAS ウイルスを直接適用すると tva を発現している細胞へのみ感染して AR2A-DN が効率よく産生，分泌される．AR2A-DN はタンパク質の産生と分泌の活性が高いので，それが循環血液中の MSTN と結合して活性を抑制し，その結果，筋分化が促進される可能性が高い．このような手順で恒常的に阻害ペプチドを供給し続ける方法であれば，筋ジストロフィーなどの筋疾患の有効な治療法になると考えられる．

　このウイルスは哺乳動物の細胞内では複製することはないので，周辺の細胞へ感染が広がる可能性はなく，レトロウイルスの感染による細胞癌化などの危険性はほとんどない．このような遺伝子治療のためのデリバリー方法は開発途上にあり，今後更なる開発が期待される．

結　　論

MSTN とその受容体の発現パターンおよび生物活性の検定から，欠損型の ActRIIA が内因性 MSTN 作用をブロックするのに最適であることの根拠が示された．これを筋分化に対する正の調節因子である Wnt ファミリーと併用することで，効果的な筋疾患の治療が可能となる．

遺伝子治療を適用するには導入遺伝子の発現効率の改善と安全性の確保が必要である．その方法として，鳥類のウイルスベクター RCAS の利用と，ウイルス受容体の遺伝子 tva の導入があり，その基礎的な発現条件の検討を行った．この方法は組換えタンパク質や抗体を全身投与する方法に比べて作用が持続的であるためより有効である．

参　考　文　献

1) 平野茂樹：ニワトリ胚子における骨格筋の発生．生体の科学　52：261－266，2001

2) Sadler TW：ラングマン人体発生学．安田峰生訳．第9版，東京，メディカル・サイエンス・インターナショナル．2005，pp 181－189

3) McPherron AC, Lawler AM, Lee SJ：Regulation of skeletal muscle mass in mice by a new TGF-β superfamily member. Nature 387：83－90, 1997

4) McPherron AC, Lee SJ：Double muscling in cattle due to mutations in the myostatin gene. Proc Natl Acad Sci USA 94：12457－12461, 1997

5) Lee SJ, McPherron AC：Regulation of myostatin activity and muscle growth. Proc Natl Acad Sci USA 98：9306－9311, 2001

6) Amthor H, Huang R, McKinnell I, et al.：The regulation and action of myostatin as a negative regulator of muscle development during avian embryogenesis. Dev Biol 251：241－257, 2002

7) Rebbapragada A, Benchabane H, Wrana JL, et al.：Myostatin signals through a transforming growth factor β-like signaling pathway to block adipogenesis. Mol Cell Biol 23：7230－7242, 2003

8) Lee SJ, Reed LA, Davies MV, et al.：Regulation of muscle growth by multiple ligands signaling through activin type II receptors. Proc Natl Acad Sci USA 102：18117－18122, 2005

9) Bogdanovich S, Krag TOB, Barton ER, et al.：Functional improvement of dystrophic muscle by myostatin blockade. Nature 420：418－421, 2002

10) Whittemore LA, Song K, LI X, et al.：Inhibition of myostatin in adult mice increase skeletal muscle mass and strength. Biochem Biophys Res Commun 300：965－971, 2003

11) Hamburger V, Hamilton H：A series of normal stages in the development of the chick embryo. J Morph 88：49－92, 1951

12) 笹岡俊輔：ニワトリ胚の四肢形成における Wnt-Frizzled 相互作用．川崎医学会誌，印刷中，2006

13) Zammit PS, Golding JP, Nagata Y, et al.：Muscle satellite cells adopt divergent fates：a mechanism for self-renewal? J Cell Biol 166：347-357, 2004

14) Goto H, Tomono Y, Ajiro K, et al.：Identification of a novel phosphorylation site on histone H3 coupled with mitotic chromosome condensation. J Biol Chem 274：25543－25549, 1999

15) Zhu X, Hadhazy M, Wehling M, et al. : Dominant negative myostatin produces hypertrophy without hyperplasia in muscle. FEBS Letters 474 : 71 − 75, 2000

16) Hill JJ, Davies MV, Pearson AA, et al. : The myostatin propeptide and the follistatin-related gene are inhibitory binding proteins of myostatin in normal serum. J Biol Chem 277 : 40735 − 40741, 2002

17) Hill JJ, Qiu Y, Hewick RM, et al. : Regulation of myostatin in vivo by growth and differentiation factor-associated serum protein-1 : A novel protein with protease inhibitor and follistatin domains. : Mol Endocrinol 17 : 1144 − 1154, 2003

18) Wolfman NM, McPherron AC, Pappano WN, et al. : Activation of latent myostatin by the BMP-1/tolloid family of metalloproteinases. Proc Natl Acad Sci USA 100 : 15842 − 15846, 2003

19) Hughes SH : The RCAS vector system. Folia Biologica (Praha) 50 : 107 − 119, 2004

20) Kawakami Y, Wada N, Nishimatsu S, et al. : Involvement of Wnt-5a in chondrogenic pattern formation in the chick limb bud. Develop Growth Differ 41 : 29 − 40, 1999

21) 山本康弘 : 顎顔面形態形成に関わる FGF-8 の解析. 川崎医学会誌 31 : 151 − 159, 2005

22) Fisher GH, Orsulic S, Holland E, et al. : Development of a flexible and specific gene delivery system for production of murine tumor models. Oncogene 18 : 5253 − 5260, 1999

23) Orsulic S : An RCAS-TVA-based approach to designer mouse models. Mammalian Genome 13 : 543 − 547, 2002

Involvement of Wnt4 Signaling During Myogenic Proliferation and Differentiation of Skeletal Muscle

Haruyuki Takata,[1] Kumiko Terada,[2] Hiroaki Oka,[1] Yoshihide Sunada,[3] Takahiko Moriguchi,[1] and Tsutomu Nohno[2]*

The direct effects of Wnt4 on myogenic proliferation and differentiation of skeletal muscle precursors are examined. *Wnt4* cDNA was misexpressed in the presumptive limb fields on the right side of stage 16 chick embryos. Muscle development was evaluated at stage 37 with hematoxylin–eosin staining and immunohistochemical staining for fast and slow types of the myosin heavy chain (MyHC). Overexpression of *Wnt4* resulted in up-regulation of *Pax7* and *MyoD1* expression. The muscle mass showed a significant increase compared with that of the control limb. The area for fast MyHC-expressing cells showed a significant increase, whereas a slight decrease was observed for slow MyHC-expressing cells. Wnt4 acted as a stimulator during myogenic proliferation and differentiation, especially for fast-type muscle in C_2C_{12} cells. The present results are identical to those of myostatin knockout, suggesting that Wnt4 is acting against myostatin as an antagonizing signal for myostatin. *Developmental Dynamics 236:2800–2807, 2007.* © 2007 Wiley-Liss, Inc.

Key words: C2C12; chick embryo; myogenesis; myosin heavy chain; myostatin; Wnt4

INTRODUCTION

Myostatin (GDF-8) is a member of the transforming growth factor (TGF) -β superfamily, acting through binding to the type II receptor for activin, ActRIIA and ActRIIB. *Myostatin* null animals are significantly larger than wild-type animals and show a great and overall increase in skeletal muscle mass (McPherron et al., 1997). Myostatin binding to ActRII elicits phosphorylation of Smad2/Smad3 through activation of type I receptors, ALK4, ALK5, and ALK7 (Rebbapragada et al., 2003; Lee et al., 2005).

Finally, myostatin acts as a specific inhibitor of skeletal muscle growth (McPherron and Lee, 1997).

However, the myostatin-responsive genes involved in skeletal muscle formation are unknown. Recently, myostatin-responsive genes in skeletal muscle were studied by microarray analysis (Steelman et al., 2006). To validate changes in gene expression identified with the microarray analysis, a real-time and quantitative polymerase chain reaction (PCR) was performed. Components involved in Wnt4 signaling were preferentially increased in the skeletal muscle after myostatin knockout, suggesting that myostatin acts upstream of Wnt4 for down-regulating Wnt4 signaling. In the adult muscle of the myostatin knockout mouse, expression of *Wnt4, Dishevelled, Calcineurin, Calmodulin kinase II, beta-catenin–binding protein,* and *Dickkopf1* was found to be increased, whereas *sFRP1, sFRP2,* and *Dickkopf2* expression was decreased (Steelman et al., 2006). Wnt4 signaling was shown to stimulate satellite cell proliferation in skeletal muscle (Steelman et al., 2006), in

agreement with the suggestion that Wnt members are known to be involved in muscular renewal after injury (Polesskaya et al., 2003).

Several Wnt molecules have been implicated as playing specific roles during vertebrate limb development, including induction of the early limb bud, formation and maintenance of a specific ectodermal structure known as the apical ectodermal ridge (AER), outgrowth of the limb, and patterning of the limb bud axes (Dealy et al. 1993; Parr et al., 1993; Kengaku et al., 1997; Galceran et al., 1999; Kawakami et al., 2001; Narita et al., 2005). *Wnt4* is expressed in the developing limb in the chick embryo, especially in the central elbow region and in the joint interzones of the wrist-forming region as early as stages 26–27. During later stages, localization of Wnt4 signals has been observed in the joint-forming regions throughout the limb (Kawakami et al., 1999, Loganathan et al., 2005).

Other members of the Wnt family are also known to regulate myogenic differentiation. Wnt signaling has been implicated in modification of the number of fast and/or slow types of myofibers. For example, Wnt11 decreases and increases the number of slow and fast myofibers, respectively, during embryogenesis, whereas Wnt5a has a reversal activity on myofiber specification (Anakwe et al., 2003).

However, the biological activity of Wnt4 in myogenic differentiation and proliferation of skeletal muscle remains unclear. We examined the myogenic effects of *Wnt4* overexpression in the limb bud to evaluate the significance of Wnt4 signaling in skeletal muscle formation during embryogenesis. Wnt4 was shown to have low but significant myogenic activity, useful for recovery from wasting of skeletal muscle in mild muscular dysfunction.

RESULTS

To analyze the potential roles of Wnt4 signaling during limb myogenic differentiation, *Wnt4* was overexpressed in the right limb muscle precursors using the RCAS vector. We first determined ectopic *Wnt4* expression with in situ hybridization at stage 28, 2 days after virus injection, and at stage 30, 4 days after virus injection. *Wnt4* was expressed in the entire right limb region at stage 28 (Figs. 1, 2A). We confirmed *Wnt4* misexpression by immunohistochemical staining for hemagglutinin (HA) tag added to the C-terminal end of Wnt4 and found similar distribution pattern for Wnt4 protein in the right limb bud as observed by in situ hybridization, 2 to 4 days after virus injection (data not shown).

To examine the effects of *Wnt4* overexpression on muscle differentiation markers, the expression patterns of the *Pax7* and *MyoD1* genes were examined with in situ hybridization on sections. *Pax7* and *MyoD1* expression in the *Wnt4*-treated right limb bud showed 1.2- to 1.3-fold and 1.6- to 2.7-fold increase, respectively, over the contralateral limb bud, when the expression area was measured and compared in the same embryo at stages 28–30 (Fig. 2B,C).

The morphology of the injected right limb was compared with that of a non-injected left limb, serving as a control. At stage 37, 7 days after injection, the thickness of the zeugopod in the injected right leg had significantly increased (Fig. 3). The knee joint (articulate) showed hyperflexion, and the ankle joint showed hyperdorsiflexion. We evaluated 23 embryos, and 18 embryos (78%) showed similar phenotypic changes. We treated a total of 51 embryos, and 28 embryos were fixed at early stages for evaluating gene expression patterns at different stages with in situ hybridization.

When we compared the maximum diameter and area of the leg on the stained sections, the muscles of the injected right limb showed an apparent increase in overall muscle size in the cross-sectioned area, compared with the contralateral limb of the controls (Fig. 4A). Fast and slow MyHC expression was examined in the leg muscles (Fig. 4B,C). The area for fast MyHC-expressing cells of the injected right limb was clearly wider than that of the contralateral limb (Fig. 4B). The area for slow MyHC-expressing cells was not significantly different but slightly decreased for the treated limbs compared with the control limb (Fig. 4C). The area for fast MyHC-expressing cells in the treated limb was significantly larger than that for the control ($P < 0.05$), whereas the area for slow MyHC-expressing cells in the treated limb was slightly smaller than that for the control, as determined by measuring the area for eight independent embryos (Fig. 5A). Consequently, the ratio of the area for fast MyHC to slow MyHC in the treated limb was significantly higher than that for the control (Fig. 5B). There was no difference in these areas compared with the contralateral limb, when enhanced green fluorescence protein (EGFP) -RCAS was injected instead of *Wnt4*-RCAS (data not shown). Thus, *Wnt4*-treated limb showed the overall increase in the muscle mass and significant increase in fast-type muscle size after *Wnt4* misexpression, accompanying elevated expressions of *Pax7* and *MyoD1*.

To confirm the role of Wnt4 during myogenic development, C_2C_{12} cells were used to transfect with *Wnt4* to analyze muscle differentiation and fiber-type specification. The number of fast MyHC-expressing cells of the cultures with overexpression of *Wnt4* showed a significant increase compared with those of the control cultures ($P < 0.01$; Figs. 6B,D, 7). A slight decrease in the number of the slow MyHC-expressing cells was observed in the cultures, with overexpression of *Wnt4* compared with those of the control cultures (Figs. 6A,C, 7), although the difference between the treated and control groups was not significant. Identical results were obtained in the similar experiments repeated three times.

To evaluate the interaction between myostatin and Wnt4 signaling, C_2C_{12} cells were transfected with *Wnt4HA* or *EGFP* in pcDNA3.2, and cultured further in the differentiation medium with or without recombinant myostatin. Western blot analysis of the total protein indicated phospho-Smad2 signal was greatly increased by myostatin addition, whereas Wnt4 expression had no effect on Smad2 phosphorylation (Fig. 8). When Wnt4 was expressed by transfection, phospho-Smad2 was not increased by myostatin addition (Fig. 8), suggesting that Wnt4 antagonizes against myostatin at Smad2/3 phosphorylation, thereby increasing myogenic proliferation and/or differentiation in C_2C_{12} myoblasts.
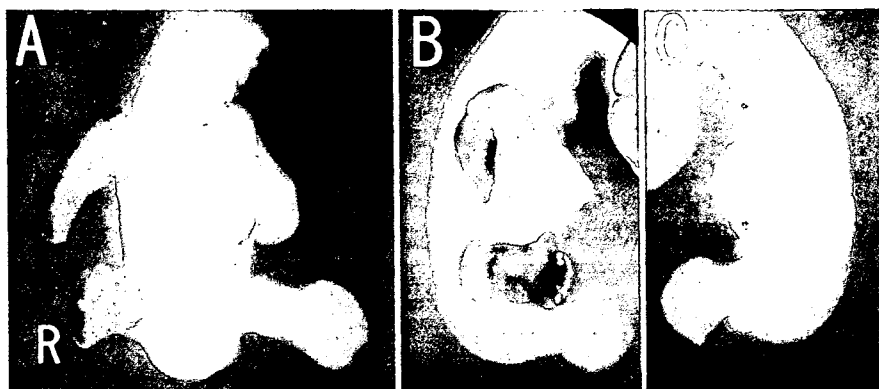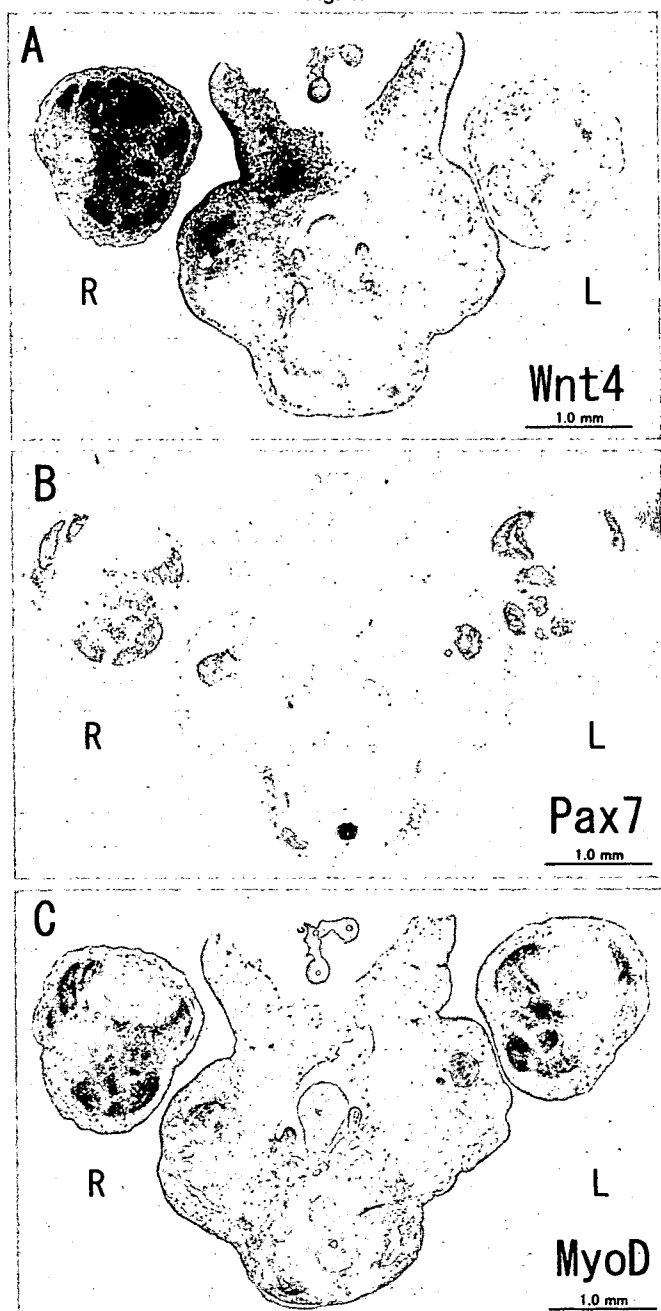
Fig. 1.

Fig. 2.

DISCUSSION

Wnt signaling is known to play a role in embryonic myogenesis (Cossu and Borello, 1999; Buckingham et al., 2003). An analysis of Wnt signaling by gain-of-function studies in vitro showed that an increase in the number of terminally differentiated cells in a *Wnt4*-transfected cell culture was associated with a significant increase in the number of slow MyHC-expressing cells (Anakwe et al., 2003). Our results showed that the number of the fast MyHC-expressing cells after *Wnt4* overexpression significantly increased, whereas the number of slow-type MyHC-expressing cells slightly decreased both in embryos and in the cell culture. Although we cannot explain the differential effects on slow-type MyHC expression after *Wnt4*, the stage of the embryo used for the assay may have an influence on responsiveness to the Wnt family.

Wnt signals are transduced through at least three distinct intracellular signaling pathways, the canonical Wnt/β-catenin pathway, the Wnt/Ca^{2+} pathway, and the Wnt/JNK pathway (Miller, 2001), although the downstream signal of Wnt4 has not been elucidated. When we assayed Wnt4 activity with a reporter assay using TOPFLASH and FOPFLASH, Wnt4 was shown to have an activity to transduce signals through the β-catenin pathway, although the activation was not as high as that observed for Wnt3a, a typical activator for the β-catenin pathway (data not shown).

The Wnt/β-catenin pathway is thought to play a critical role in em-

Fig. 1. Whole-mount in situ hybridization of *Wnt4* at stage 28, 2 days after *Wnt4*-RCAS injection into the right limb bud at stage 16. A: Ventral view. B: Right side view. C: Left side view. R, right (treated).

Fig. 2. Expression of *Wnt4*, *Pax7*, and *MyoD1* at stage 30, 4 days after *Wnt4*-RCAS injection into the right limb bud at stage 16. A transverse section at the middle of the hindlimb on the anterior–posterior limb axis. Ventral is on the top. The left hindlimb is the control for the right hindlimb infected with *Wnt4*-RCAS. A: Expression of *Wnt4*. The *Wnt4* signals dramatically increased in the right limb. B: Expression of *Pax7*. C: Expression of *MyoD1*. Both signals significantly increased in the right limb (B,C). Scale bars = 1 mm in A–C.
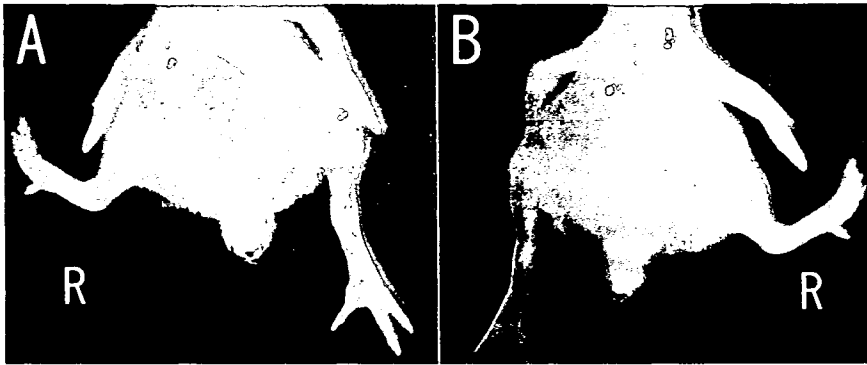
Fig. 3. Phenotypic changes in the right limb at stage 37, 10 days after *Wnt4*-RCAS injection into the right limb bud at stage 16. **A:** Ventral view. **B:** Dorsal view. R, right.
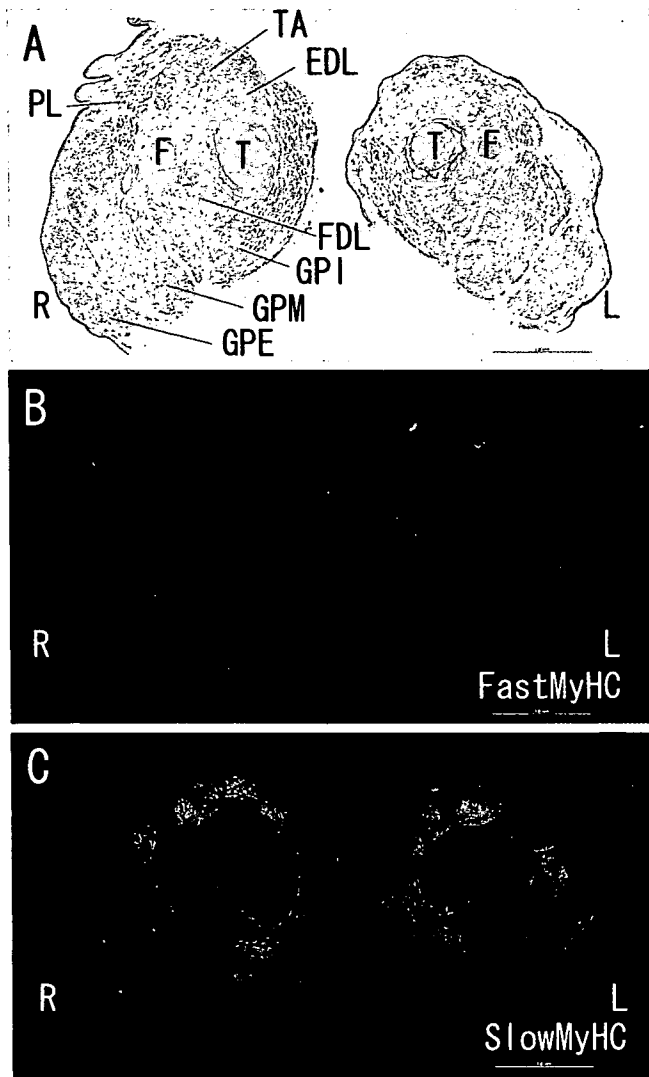

Fig. 4. Effect of overexpression of *Wnt4* on fiber-type differentiation in the chick embryo. **A–C:** Hematoxylin–eosin staining (A) and fluorescent images (B,C) of a transverse section of the stage 37 chick hindlimb that was infected with *Wnt4*-RCAS in the right hindlimb. **B:** Leg section was visualized for fast myosin heavy chain (MyHC). **C:** Leg section was visualized for slow MyHC. R, right; L, left; F, fibula; T, tibia; TA, tibialis anterior; EDL, extensor digitorum longus; FDL, flexor digitorum longus; GPE, gastrocnemius pars externa; GPI, gastrocnemius pars interna; GPM, gastrocnemius pars media; PL, peroneus longus. Scale bars = 1 mm in A–C.

bryonic myogenesis (Petropoulos and Skerjanc, 2002; Pan et al., 2005). Blocking the β-catenin pathway reduced the total number of myocytes, and this effect was associated with a significant decrease in the number of cells expressing fast MyHC. Nevertheless, overexpression of *Wnt3a* has significantly decreased the number of terminally differentiated myogenic cells (Anakwe et al., 2003). When active *Wnt3a* was overexpressed, the limb became malformed due to inhibitory effect on chondrogenesis, in addition to the ectopic AER formation (Narita et al., 2007). Both the β-catenin pathway and another noncanonical pathway are probably necessary for proper myogenic differentiation.

Wnt4 signaling inhibits testosterone biosynthesis by repressing SF1/β-catenin synergy (Jordan et al., 2003) and acts to regulate sex determination (Kim et al., 2006). Because androgens, including testosterone, are known to have anabolic activity to stimulate myogenesis, inhibition of testosterone biosynthesis is not involved in myogenesis after *Wnt4* misexpression.

Wnt4 is expressed in the central elbow region and in the joint interzones of the wrist-forming region at stages 26–27, and in the joint-forming regions of the limb bud at later stages (Kawakami et al., 1999; Loganathan et al., 2005). Hyperflexion phenotypes of the leg after *Wnt4* misexpression may not be derived from the effects on chondrogenesis in the knee and ankle joint (Hartmann and Tabin, 2000). Endogenous *Wnt4* expression was not detected in the proximity of the muscle-forming region during limb development (Kawakami et al., 1999). Although there is no direct evidence for *Wnt4* expressed at a far distance, Wnt4 emanating from the joint-forming region may affect myogenic differentiation in the surrounding region, thereby affecting overall leg shape.

Myostatin is an inhibitor of skeletal muscle growth. Follistatin, a myostatin propeptide (Hill et al., 2002, 2003; Wolfman et al., 2003), a neutralizing antibody (Whittemore et al., 2003), and a dominant-negative receptor (Lee et al., 2005) have been used to block the function of myostatin. We have also previously examined the effect of dominant-negative *ActRIIA* and *ActRIIB* during skeletal muscle
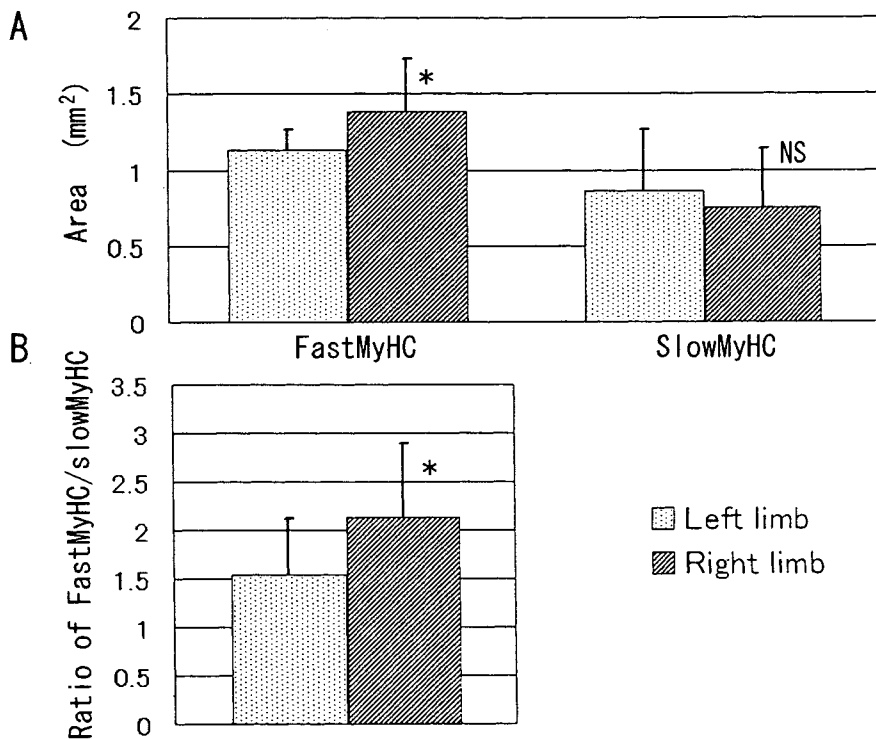
Fig. 5. The effect of *Wnt4* overexpression on fiber-type differentiation in the chick embryo. **A:** Area of muscle cells expressing fast or slow myosin heavy chain (MyHC) in a transverse section in the chick hindlimb at stage 37. **B:** Ratio of fast/slow MyHC-expressing area. Results are shown as mean ± standard deviation of eight independent embryos. *$P < 0.05$; NS, not significant.

development by using a retrovirus vector to misexpress in the chick embryos (Takata et al., 2006). A stimulatory effect of myogenic differentiation was observed in myoblast cell cultures, although no significant effect was obtained in vivo. Because Wnt4 is presumed to be a downstream signal of myostatin, a more intense and direct effect is anticipated after overexpression of *Wnt4* to stimulate myogenic differentiation and proliferation during embryogenesis.

Although Wnt4 was found to act as a stimulator during myogenic proliferation and/or differentiation, especially, for fast-type muscles, increased muscle masses in *Wnt4*-expressing limb compared with the control limb may be due to hypertrophy of the muscle cells, rather than increased proliferation. An increase in the cell number of fast MyHC-expressing C_2C_{12} cells may indicate the extent of differentiation to fast-type myofiber, not necessary indicating increased cell proliferation. The present results using *Wnt4* misexpression are identical to those for myostatin knockout (Girgenrath et al., 2005), because the soleus of myostatin knockout mice displays large proportion of fast type II fibers and a reduced proportion of slow type I fibers compared with wild-type mice. *Wnt4* misexpression resulted in the similar phenotype on fiber type differentiation in C_2C_{12} cells, and, therefore, Wnt4 is considered to
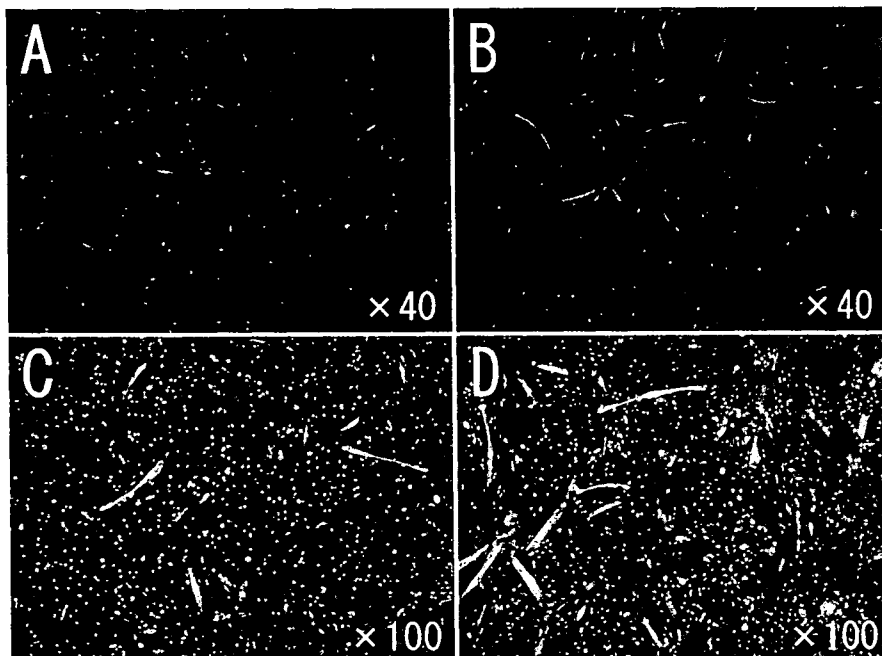

Fig. 6. Effect of overexpression of *Wnt4* on fiber-type differentiation in cultured C_2C_{12} myoblasts. **A,C:** *EGFP* was transfected in cell cultures as a control. **B,D:** *Wnt4* was transfected in cell cultures. Fluorescent images showing terminally differentiated C_2C_{12} that has been visualized with antibodies recognizing fast myosin heavy chain (MyHC; red) and slow MyHC (green). Original magnification, ×40 in A,B, ×100 in C,D.
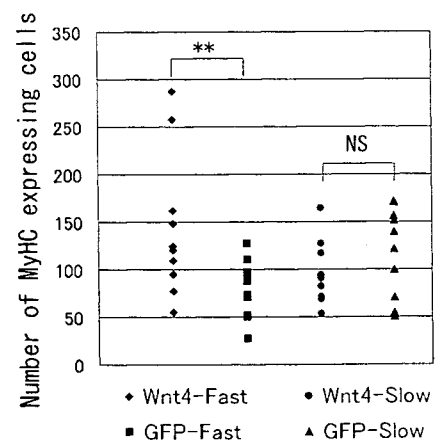

Fig. 7. Effect of overexpression of Wnt4 on fiber-type differentiation in cultured C_2C_{12} myoblasts. The dot shows the number of fast and slow myosin heavy chain (MyHC) -expressing cells in cultures that have been transfected with *Wnt4* or *EGFP*. Mean ± standard deviation (n = 10). **$P < 0.01$; NS, not significant.
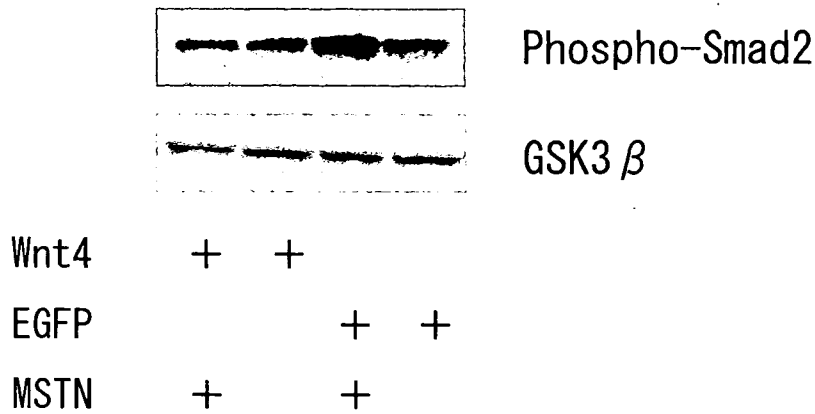
Fig. 8. Western blot analysis of phospho-Smad2 in C_2C_{12} cells expressing *Wnt4* or *EGFP* in the presence or absence of recombinant myostatin. Expression constructs for *Wnt4HA* and *EGFP* were introduced into C_2C_{12} myoblasts by transfection, and myostatin (500 ng/ml) or vehicle was added to the differentiation medium for 48 hr. Total proteins (45 μg per lane) were used for electrophoresis and detected with anti–phospho-Smad2 and anti-GSK3β antibodies after blotting.

act against myostatin primarily on fast-type muscles, as presumed by microarray analysis (Steelman at al., 2006).

However, the results on phospho-Smad2 suggest signal cross-talk between the myostatin pathway and Wnt4 pathway (Fig. 8). Although much works need to be done to find out details on the interaction, both myostatin inhibition and Wnt4 activation are useful to increase myogenesis, especially for fast-type myofiber.

EXPERIMENTAL PROCEDURES

Chicken Embryos

Fertilized specific pathogen-free White Leghorn eggs were obtained from Nisseiken (Oume, Japan), and incubated at 38°C in a humidified atmosphere. The embryos were staged according to Hamburger and Hamilton (1951).

Plasmid Construction

Chick *Wnt4* cDNA (Tanda et al., 1995) was used for subcloning into expression vectors. *EGFP* cDNA was obtained from Wako Chemicals as green fluorescent protein (GFP) pQBI-polII. To overexpress *Wnt4* and *EGFP* cDNAs in C_2C_{12} cells, these genes were subcloned into pcDNA3.2DEST (Invitrogen, Carlsbad, CA). An HA-tag was added to the C-terminal of *Wnt4* using mouse *Wnt3a* cDNA in pUSE-amp (Upstate, Temecula, CA) that contains the HA-tag sequence at the

C-terminal end, after restriction subcloning to replace the full-coding sequence of *Wnt3a* with *Wnt4*. To carry out misexpression in the developing limb bud, the full coding sequences of *Wnt4HA* and *EGFP* were subcloned into RCAS (Hughes et al., 1987).

In Situ Hybridization

We examined the expression of the *Wnt4*, *Pax7*, and *MyoD1* genes with section and whole-mount in situ hybridization. Embryos were fixed in 4% paraformaldehyde (PFA) in phosphate-buffered saline (PBS) at 4°C overnight and dehydrated in ethanol. Whole-mount in situ hybridization was performed as described using *Wnt4* cDNA and other cDNAs as templates for probes (Kawakami et al., 1999). Dehydrated embryos were embedded in paraffin and sectioned with a microtome at 7-μm thicknesses.

Section in situ hybridization was performed as described previously (Ito et al., 2007). Chicken *MyoD1* cDNA was generously obtained from A. Kuroiwa (Yamamoto and Kuroiwa, 2003). Chicken *Pax7* cDNA was amplified with a PCR using the following primers based on the chicken *Pax7* sequence (accession no. NM_205065): 5'-CACCATG-GCAGCGCTCCCCGGGA-3' and 5'-TCAGTAAGCTTGGCCTGTCTCC-3'. The amplified cDNA was cloned into pCRII-D-TOPO and identified by sequencing.

Misexpression in the Chick Limb Bud

To prepare recombinant viral particles, the RCAS construct was transfected into DF-1 cells (ATCC; #CRL-12203) using Lipofectamine 2000 (Invitrogen). Cells were grown in the culture medium (2% fetal bovine serum [FBS] and 1% chicken serum in Dulbecco's modified eagle medium [D-MEM]). After confluence in a 2-cm culture dish, it was replaced with 2 ml of fresh medium (2% FBS and 1% chicken serum in D-MEM). On the next day, the medium was replaced and harvested as primary viral stock. After medium replacement four times, the medium was pooled. To concentrate the virus particles in the culture medium, it was centrifuged at 4°C for 10 min at 20,000 rpm to remove cell debris. The clear supernatant was transferred into a new centrifugation tube, and centrifuged again at 4°C for 2 hr at 20,000 rpm. After the major part of the medium was discarded by aspiration, the virus particles in the bottom pellet were resuspended in a small volume of the remaining medium (approximately 200 μl). The retrovirus was injected into the presumptive limb fields on the right side of embryos at stages 15–17 with a microinjector (IM-300, NARISHIGE, Japan). After 2 to 4 days of reincubation, the embryos were fixed in 4% PFA in PBS and the gene expression pattern was determined using in situ hybridization. Seven days after injection, embryos were sectioned in a parallel position to prepare equivalent sections along the proximodistal axis for the right and left legs, which served as treated and control limbs, respectively. As a control experiment, we used *EGFP*-RCAS in place of *Wnt4*-RCAS for transfection and misexpression.

Cell Culture and Transfection Assay

The C_2C_{12} cell line (myoblast-like cell line from C3H mouse) was obtained from RIKEN Cell Bank (RIKEN, Wako, Japan; Yaffe and Saxel, 1977; Blau et al., 1983). Cells were propagated in the culture medium (10% FBS in D-MEM). At 12–24 hr after subculturing, transfection was per-

formed using Lipofectamine 2000 reagent according to the manufacturer's instruction (Invitrogen). C_2C_{12} cells were transfected with 2 μg of *Wnt4HA* or *EGFP* in pcDNA3.2 in 2-ml culture dish (35 mm diameter). The transfected cells were cultured in a differentiation medium containing 2% horse serum in D-MEM. After further culturing for 72 hr, cells were fixed and then immunohistochemically stained for fast-type MyHC and slow-type MyHC.

Western Blot Analysis

Cells were propagated in the culture medium (10% FBS in D-MEM). At 24 hr after subculturing, C_2C_{12} cells were transfected with 10 μg of *Wnt4HA* or *EGFP* in pcDNA3.2 in 10-ml culture dish (100-mm diameter). The transfected cells were cultured in a differentiation medium containing 2% horse serum in D-MEM. At 24 hr after transfection, 500 ng/ml of recombinant myostatin (R&D Systems, Minneapolis, MN) or vehicle was added. After further culturing for 48 hr, cells were harvested and used to prepare total protein extracts. Western blotting was performed as described previously (Ito et al., 2007). Rabbit anti–phospho-Smad2 antibody (Ser465/467; Cell Signaling, Danvers, MA) was used as primary antibodies at dilutions of 1:1,000 by incubating overnight at 4°C. To estimate protein recovery during preparation, rabbit anti-GSK3β antibody (H-76; Santa Cruz, CA) was used as the primary antibody at a dilution of 1:200. Peroxidase-linked anti-rabbit IgG antibody (Amersham Biosciences, Buckinghamshire, UK) was used as the secondary antibody for chemiluminescence detection.

Immunohistochemistry

Dehydrated embryos were embedded in paraffin and sectioned with a microtome at 5 μm. Immunohistochemical staining of sections was performed with the VENTANA HX SYSTEM Discovery (VENTANA Medical Systems, Tucson, AZ). Muscle differentiation was estimated by immunohistochemical staining using the following primary antibodies; anti-slow MyHC antibody (M8421, Sigma-Aldrich, St.

Louis, MO) with a 1:200 dilution in PBS, and anti-fast MyHC antibody (M4276, Sigma-Aldrich) with a 1:100 dilution in PBS. After 60-min incubation, slides were washed and treated with Alexa Fluor–conjugated goat anti-mouse IgG (A11032, Molecular Probes, Eugene, OR) with a 1:200 dilution in PBS. The data were analyzed using IPLab/Win Version 3.6.5a (Scanalytics).

Cell cultures were fixed in ethanol:formalin:acetic acid:H_2O (14:2:1:6, v/v) at room temperature for 10 min. After washing three times with PBS, cells were treated with 2% goat serum, 2% skim milk, 0.2% Tween20 in Tris-buffered saline (TBS; 50 mM Tris-HCl, pH 7.5, 150 mM NaCl) at room temperature for 30 min. Then the first primary antibody, anti-fast MyHC antibody (M4276, Sigma-Aldrich) was used with a 1:400 dilution in PBS at 4°C overnight. After washing three times with TBS, the first secondary antibody, Alexa Fluor 594–conjugated goat anti mouse IgG (A11032, Molecular Probes, Invitrogen) was used with a 1:200 dilution in PBS at room temperature for 60 min. After washing three times with TBS, the second primary antibody, anti-slow MyHC antibody (M8421, Sigma-Aldrich) was used with a 1:1,000 dilution in PBS at 4°C overnight. Then, after washing three times with TBS, the second secondary antibody, fluorescein isothiocyanate–conjugated rabbit anti-mouse IgG (F9137, Sigma-Aldrich) was used with a 1:200 dilution in PBS at room temperature for 60 min. The nuclei were stained with 1 μg/ml 4',6-diamino-2-phenylindole solution (DOJINDO, Japan).

For statistical evaluation of muscle differentiation, the numbers of nuclei in the MyHC-positive cells were counted in three different randomly chosen views of 10 independent cultures.

REFERENCES

Anakwe K, Robson L, Hadley J, Buxton P, Church V, Allen S, Hartmann C, Harfe B, Nohno T, Brown AM, Evans DJ, Francis-West P. 2003. Wnt signalling regu-

lates myogenic differentiation in the developing avian wing. Development 130:3503–3514.

Blau HM, Chiu CP, Webster C. 1983. Cytoplasmic activation of human nuclear genes in stable heterocaryons. Cell 32:1171–1180.

Buckingham M, Bajard L, Chang T, Daubas P, Hadchouel J, Meilhac S, Montarras D, Rocancourt D, Relaix F. 2003. The formation of skeletal muscle: from somite to limb. J Anat 202:59–68.

Cossu G, Borello U. 1999. Wnt signaling and the activation of myogenesis in mammals. EMBO J 18:6867–6872.

Dealy CN, Roth A, Ferrari D, Brown AM, Kosher RA. 1993. Wnt-5a and Wnt-7a are expressed in the developing chick limb bud in a manner suggesting roles in pattern formation along the proximodistal and dorsoventral axes. Mech Dev 43:175–186.

Galceran J, Farinas I, Depew MJ, Clevers H, Grosschedl R. 1999. Wnt 3a(−/−)-like phenotype and limb deficiency in Lef 1(−/−) Tcf 1(−/−) mice. Genes Dev 13:709–717.

Girgenrath S, Song K, Whittemore LA. 2005. Loss of myostatin expression alters fiber-type distribution and expression of myosin heavy chain isoforms in slow- and fast-type skeletal muscle. Muscle Nerve 31:34–40.

Hamburger V, Hamilton HL, 1951. A series of normal stages in the development of the chick embryo. J Morphol 88:49–92.

Hartmann C, Tabin CJ. 2000. Dual roles of Wnt signaling during chondrogenesis in the chicken limb. Development 127:3141–3159.

Hill JJ, Davies MV, Pearson AA, Wang JH, Hewick RM, Wolfman NM, Qiu Y. 2002. The myostatin propeptide and the follistatin-related gene are inhibitory binding proteins of myostatin in normal serum. J Biol Chem 277:40735–40741.

Hill JJ, Qiu Y, Hewick RM, Wolfman NM. 2003. Regulation of myostatin in vivo by growth and differentiation factor-associated serum protein-1: a novel protein with protease inhibitor and follistatin domains. Mol Endocrinol 17:1144–1154.

Hughes SH, Greenhouse JJ, Petropoulos CJ, Sutrave P. 1987. Adaptor plasmids simplify the insertion of foreign DNA into helper-independent retroviral vectors. J Virol 61:3004–3012.

Ito S, Honma T, Ishida K, Wada N, Sasaoka S, Hosoda M, Nohno T. 2007. Differential expression of the human α-enolase gene in oral epithelium and squamous cell carcinoma. Cancer Sci 98:499–505.

Jordan BK, Shen JH, Olaso R, Ingraham HA, Vilain E. 2003. Wnt4 overexpression disrupts normal testicular vasculature and inhibits testosterone synthesis by repressing steroidogenic factor 1/beta-catenin synergy. Proc Natl Acad Sci U S A 100:10866–10871.

Kawakami Y, Wada N, Nishimatsu S, Ishikawa T, Noji S, Nohno T. 1999. Involvement of Wnt-5a in chondrogenic pattern

formation in the chick limb bud. Dev Growth Differ 41:29–40.

Kawakami Y, Capdevila J, Buscher D, Itoh T, Rodriguez Esteban C, Izpisua Belmonte JC. 2001. WNT signals control FGF-dependent limb initiation and AER induction in the chick embryo. Cell 104: 891–900.

Kengaku M, Twombly V, Tabin C. 1997. Expression of Wnt and frizzled genes during chick limb bud development. Cold Spring Harb Symp Quant Biol 62:421–429.

Kim Y, Kobayashi A, Sekido R, DiNapoli L, Brennan J, Chaboissier MC, Poulat F, Behringer RR, Lovell-Badge R, Capel B. 2006. Fgf9 and Wnt4 act as antagonistic signals to regulate mammalian sex determination. PLoS Biol 4:e187.

Lee SJ, Reed LA, Davies MV, Girgenrath S, Goad ME, Tomkinson KN, Wright JF, Barker C, Ehrmantraut G, Holmstrom J, Trowell B, Gertz B, Jiang MS, Sebald SM, Matzuk M, Li E, Liang LF, Quattlebaum E, Stotish RL, Wolfman NM. 2005. Regulation of muscle growth by multiple ligands signaling through activin type II receptors. Proc Natl Acad Sci U S A 102: 18117–18122.

Loganathan PG, Nimmagadda S, Huang R, Scaal M, Christ B. 2005. Comparative analysis of the expression patterns of Wnts during chick limb development. Histochem Cell Biol 123:195–201.

McPherron AC, Lee SJ. 1997. Double muscling in cattle due to mutations in the myostatin gene. Proc Natl Acad Sci U S A 94:12457–12461.

McPherron AC, Lawler AM, Lee SJ. 1997. Regulation of skeletal muscle mass in mice by a new TGF-beta superfamily member. Nature 387:83–90.

Miller JR. 2001. The Wnts. Genome Biol 3:reviews3001.

Narita T, Sasaoka S, Udagawa K, Ohyama T, Wada N, Nishimatsu S, Takada S, Nohno T. 2005. Wnt10a is involved in AER formation during chick limb development. Dev Dyn 233:282–287.

Narita T, Nishimatsu S, Wada N, Nohno T. 2007. A Wnt3a variant participates in chick apical ectodermal ridge formation: distinct biological activities of Wnt3a splice variants in chick limb development. Dev Growth Differ 49:493–501.

Pan W, Jia Y, Wang J, Tao D, Gan X, Tsiokas L, Jing N, Wu D, Li L. 2005. β-catenin regulates myogenesis by relieving I-mfa-mediated suppression of myogenic regulatory factor in P19 cells. Proc Natl Acad Sci U S A 102:17378–17383.

Parr BA, Shea MJ, Vassileva G, McMahon AP. 1993. Mouse Wnt genes exhibit discrete domains of expression in the early embryonic CNS and limb buds. Development 119:247–261.

Petropoulos H, Skerjanc IS. 2002. β-catenin is essential and sufficient for skeletal myogenesis in P19 cells. J Biol Chem 277:15393–15399.

Polesskaya A, Seale P, Rudnicki MA. 2003. Wnt signaling induces the myogenic specification of resident CD45+ adult stem cells during muscle regeneration. Cell 113:841–852.

Rebbapragada A, Benchabane H, Wrana JL, Celeste AJ, Attisano L. 2003. Myostatin signals through a transforming growth factor beta-like signaling pathway to block adipogenesis. Mol Cell Biol 23:7230–7242.

Steelman CA, Recknor JC, Nettleton D, Reecy JM. 2006. Transcriptional profil-

ing of myostatin-knockout mice implicates Wnt signaling in postnatal skeletal muscle growth and hypertrophy. FASEB J 20:580–582.

Takata H, Terada K, Yamamoto Y, Sasaoka S, Udagawa K, Wada N, Moriguchi T, Nohno T. 2006. Myogenic activity of the dominant-negative form of type II receptor for myostatin during skeletal muscle development (abstract in English). Kawasaki Med J 32:175–186.

Tanda N, Kawakami Y, Saito T, Noji S, Nohno T. 1995. Cloning and characterization of Wnt-4 and Wnt-11 cDNAs from chick embryo. DNA Sequence 5:277–281.

Whittemore LA, Song K, Li X, Aghajanian J, Davies M, Girgenrath S, Hill JJ, Jalenak M, Kelley P, Knight A, Maylor R, O'Hara D, Pearson A, Quazi A, Ryerson S, Tan XY, Tomkinson KN, Veldman GM, Widom A, Wright JF, Wudyka S, Zhao L, Wolfman NM. 2003. Inhibition of myostatin in adult mice increases skeletal muscle mass and strength. Biochem Biophys Res Commun 300:965–971.

Wolfman NM, McPherron AC, Pappano WN, Davies MV, Song K, Tomkinson KN, Wright JF, Zhao L, Sebald SM, Greenspan DS, Lee SJ. 2003. Activation of latent myostatin by the BMP-1/tolloid family of metalloproteinases. Proc Natl Acad Sci U S A 100:15842–15846.

Yaffe D, Saxel O. 1977. Serial passaging and differentiation of myogenic cells isolated from dystrophic mouse muscle. Nature 270:725–727.

Yamamoto M, Kuroiwa A. 2003. Hoxa-11 and Hoxa-13 are involved in repression of MyoD during limb muscle development. Dev Growth Differ 45:485–498.

【TGF-βファミリーシグナルによる神経・筋疾患の制御】

TGF-β superfamily signaling in neuromuscular disorders

大澤　裕・砂田　芳秀

Oosawa　Yutaka　　Sunada　Yoshihide

要　約

　神経・筋疾患の分子病態におけるTGF-βファミリーシグナルの異常と，これを標的とした新規治療法について紹介する。アルツハイマー病患者脳では，TGF-β1遺伝子発現量とTGF-β1 typeII 受容体（TβRII）蛋白量が減少し，認知症の重症度と相関している。ニューロンにおけるTβRIIの減少は，βアミロイド蛋白質の沈着を増加させ，ニューロンの変性死を促進することから，アルツハイマー病の発症機序にTGF-β1シグナルの抑制が関与している可能性がある。Duchenne 型筋ジストロフィー(DMD)モデルマウスでは，骨格筋のTGF-β1シグナルが亢進しており，高血圧治療薬であるアンギオテンシンIIタイプ1受容体（AT1R）阻害剤Losartanを投与してTGF-β1シグナルを是正すると，病態が著明に改善する。また骨格筋特異的なTGF-βスーパーファミリーであるマイオスタチンは骨格筋萎縮を促進し，その阻害療法によってDMDモデルマウスの病態が改善し，現在，筋ジストロフィー患者での臨床治験が進行中である。

はじめに

　TGF-βファミリーシグナルについては，培養系の確立している未分化な細胞を用いて，細胞周期の制御および発がんの機構といった様々な観点から研究が進行してきた。一方，ニューロンおよび骨格筋細胞といった高度に分化した細胞でのこのシグナルの役割については，最近まで殆ど明らかでなかった。ところが，近年，このシグナルの異常が，神経・筋疾患おいて重要な役割を果たしていることが解明され，現在このシグナル異常の是正を目標とした新規治療法の開発が注目されている。

1.　アルツハイマー病とTGF-β1シグナル

　アルツハイマー病は，最も頻度の高い認知症の原因疾患で，脳実質へのアミロイドβ（Aβ）蛋白質の異常沈着（老人斑）と，ニューロンの変性死を病理学的特徴とする。脳実質の老人斑の量と認知症の進行度が相関することから，Aβ蛋白質の異常沈着は認知症発症のトリガーイベントと考えられている。しかし，なぜAβ蛋白質が異常沈着するのか，なぜAβ蛋白質の異常沈着によってニューロンが変性死に陥るのかという病態機構については，依然として全容が解明されていない。

　2001年，アルツハイマー病の老人斑のAβ蛋白質染色性と大脳皮質のTGF-β1 mRNA量とに逆相関があること，TGF-β1 の添加によって培養ミクログリアに発現させたAβ蛋白質の発現抑制が認められることが報告され，TGF-β1 シグナルがアルツハイマ

<Normal brain>

TGF-β1

Type II
Receptor
(TβRII)

Aβ deposition
neuronal loss

**Progression of
Alzheimer's disease**

<Alzheimer brain>

TGF-β1

Type II
Receptor
(TβRII)

Aβ deposition
neuronal loss

**Progression of
Alzheimer's disease**

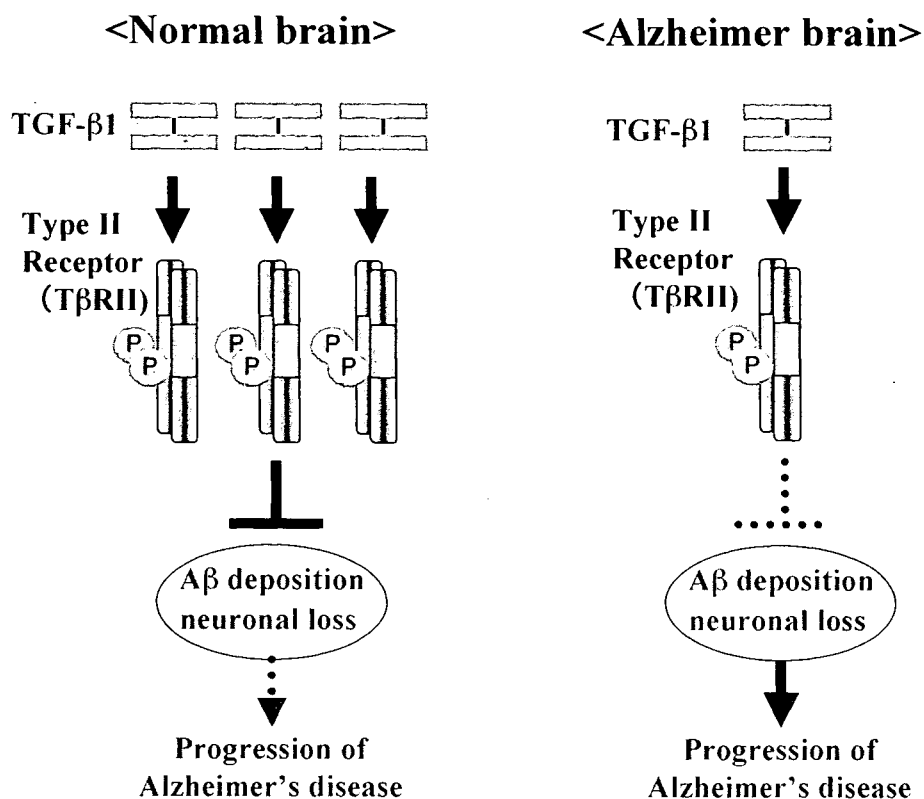図1　正常脳では，TGF-β1は，ニューロンのTypeII受容体（TβRII）に結合して，Aβの沈着とニューロン変性死を抑制している。一方，Alzheimer病患者脳では，TGF-β1とニューロンのTGF-β1のType II受容体（TβRII）発現が減少し，Aβの沈着とニューロン変性死が促進している。

一病脳のAβ蛋白質の異常沈着に対して抑制的に働いているのではないかと考えられるようになった[1]。

2006年Tesseurらは[2]，TGF-β1の膜受容体であるtype II受容体（TβRII）が，大脳皮質及び海馬ニューロンで発現していることを報告した。彼らは正常対照老人脳と比較してアルツハイマー病患者脳ではTβRII蛋白量が有意に減少し，認知症進行度と相関することを明らかにした。さらにTβRIIの条件付きノックアウトマウスを作出すると，このマウスの大脳皮質および海馬でニューロンの変性死が促進されていた。そこで，このTβRIIノックアウトマウスとAβの前駆体であるアミロイド前駆蛋白質（APP）を高発現したトランスジェニックマウスとを交配しTβRII欠損/APP高発現マウスを作出し解析したところ，大脳及び海馬でAbの沈着が有意に増加しニューロン数は有意に減少していた。

これらの結果からは，アルツハイマー病では何らかの原因によって脳内のTGFβ1やニューロンのTβRIIといったTGF-β1シグナルの抑制がおこり，次いでAβの異常沈着が引き起こされ，最後にニュ

ーロンの変性死がおこるという疾患パラダイムが考えられる。

2.　筋ジストロフィーとTGF-β1シグナル

TGF-β1が，種々の筋ジストロフィー患者の血清で上昇しており，筋衛星細胞および筋芽細胞の融合・分化を抑制することが知られていたが，その意義については長らく不明であった。

2007年ジョンホプキンス大学の循環器疾患研究グループは，高血圧治療薬として臨床で広く使われているアンギオテンシンIIタイプ1受容体（AT1R）阻害薬Losartanが，TGF-β1シグナルを抑制することによってMarfan症候群に伴うミオパチーおよびDuchenne型筋ジストロフィー（DMD）モデルであるmdxマウスの骨格筋病変を著明に改善させると報告した[3]。Marfan症候群は細胞外マトリックス構成蛋白質であるfibrillin-1の遺伝子変異により発病するが，運動負荷しても骨格筋肥大がおこらないというユニークな臨床症状を呈する。疾患モデル動物であ
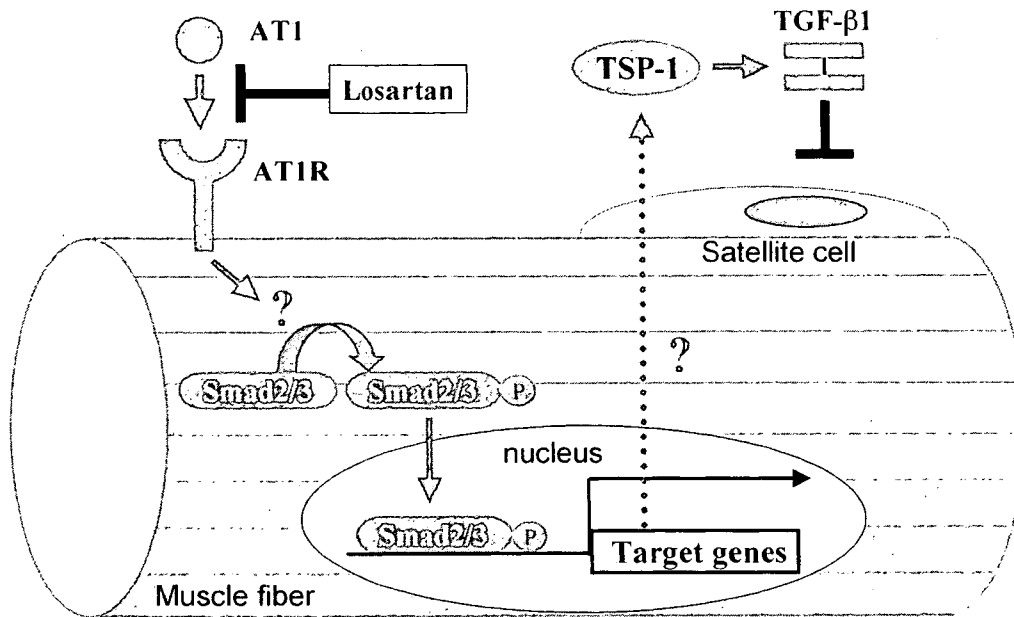
図2　高血圧治療薬Losartanは、TGF-β1シグナル亢進の認められる変異fibrillin-1トランスジェニック（Marfan症候群モデル）マウス及びdystrophin欠損筋ジストロフィー(Duchenne型)モデルマウスの骨格筋病変を改善する。こうした病的骨格筋ではTGF-β1エフェクターであるSmad2/3のリン酸化亢進とTGF-β1 activatorであるTSP-1の発現亢進が認められる（↑）。高血圧治療薬Losartan投与は、AT1とAT1Rの結合を抑制することによりSmad2/3のリン酸化抑制及びTSP-1発現抑制によって、TGF-β1シグナルを抑制し、筋衛星細胞（satellite cell）による筋再生を促進する。

る変異fibrillin-1高発現トランスジェニックマウスでは、肺においてTGF-β1シグナルの活性化に伴って肺気腫が生じることが知られていた[4]。

彼らは、まず、Marfan症候群モデルマウスの萎縮骨格筋においてTGF-βファミリーシグナルの細胞内エフェクターであるSmad2/3のリン酸化亢進（活性化）がおこっていることを確認し、次いでこのマウスにTGF-β1阻害中和抗体を腹腔内投与すると、亢進していたSmad2/3のリン酸化が減少・正常化するとともに、ミオパチーも改善することを証明した。すなわちMarfan症候群では、fibrillin-1遺伝子変異によって骨格筋のTGF-β1シグナルが活性化し、ミオパチーに至るという病態機構が考えられた。一方、高血圧治療薬であるAT1R阻害薬Losartanは、TGF-β1遺伝子発現を抑制することによって尿毒症モデルラットの腎病変および心筋症モデルマウスの心筋病変を改善することが知られていた。そこで彼らは、LosartanがTGF-β1シグナルの活性化したMarfan症候群モデルマウスの骨格筋病変をも改善するのではないかと仮定し、モデルマウスにLosartanを長期間

経口投与した。投与マウスではミオパチーが著明に改善し、骨格筋ではSmad2/3のリン酸化が抑制され正常化するばかりでなく、TGF-β1活性促進蛋白質であるThrombospondin-1（TSP-1）発現も著明に抑制された。

このグループは、引き続きdystrophin欠損筋ジストロフィーモデルマウスに対するLosartanの治療効果についても検討した。まずモデルマウスで、Smad2/3のリン酸化亢進、TSP-1発現上昇があることを確認し、6週齢モデルマウスに、飲水に混ぜたLosartan（0.5 g Losartan /l）を9ヶ月間投与した。著明な骨格筋量の増加と、筋線維萎縮の改善、間質線維化の減少、及び運動機能の改善が認められた。免疫組織学的解析では、Smad2/3のリン酸化レベルTSP-1発現レベルともほぼ正常化していた。

TGF-β1阻害中和抗体およびLosartanによるTGF-β1シグナル抑制が、どのような分子機序でミオパチーおよび筋ジストロフィーモデルマウスの骨格筋病変を改善するのか、彼らは骨格筋線維の形質膜を破壊する蛇毒であるcardiotoxinを用いて解析した。